Journal of Solid State Chemistry 184 (2011) 1655–1660

Contents lists available at ScienceDirect

Journal of Solid State Chemistry

journal homepage: www.elsevier.com/locate/jssc

The ability of RP-type cobaltites to accommodate carbonate groups: A new layered oxide $Sr_4Co_2(CO_3)O_{5.86}$

A. Demont [a], D. Pelloquin [a,*], S. Hébert [a], Y. Bréard [a], J. Höwing [b], Y. Miyazaki [c], A. Maignan [a]

[a] Laboratoire CRISMAT, UMR CNRS-ENSI Caen 6508, 6 bd Maréchal Juin, 14050 CAEN Cedex, France
[b] Instituttveien 18, 2007 Kjeller, Norway
[c] Graduate School of Engineering, Tohoku University, 6-6-05 Aoba Aramaki, Aoba-ku, Sendai 980-8579, Japan

ARTICLE INFO

Article history:
Received 12 January 2011
Received in revised form
15 March 2011
Accepted 4 April 2011
Available online 22 April 2011

Keywords:
Cobaltite
Oxycarbonate
Powder neutron diffraction data
Transmission electron microscopy

ABSTRACT

The possibility to introduce carbonate groups inside a pure cobalt based Ruddlesden Popper type matrix is demonstrated. This paper reports the synthesis as a single phase of a new layered oxycarbonate $Sr_4Co_2(CO_3)O_{5.86}$ and its structural characterizations at room temperature combining TEM observations and powder neutron diffraction data. Close structural relationships are observed with the homologous $Sr_4Fe_{3-x}(CO_3)_xO_{10-4x}$ series and deal with the presence of two specific carbonate configurations, namely coat hanger and flag. Magnetization measurements reveal a complex antiferromagnetic behavior below 50 K with three others transitions, at 160, 210 and 250 K. Such behavior can be ascribed to the latent reactivity in air of this largely oxygen deficient phase.

1. Introduction

The importance of layering to generate transition-metal oxides with 2D structures has been illustrated in the last decades by the high T_C of superconducting cuprates containing CuO_2 [1] planes, the low T_C of the superconducting hydrated cobaltite $Na_{0.3}CoO_2$, $1.3H_2O$ [2] or the importance of Li_xCoO_2 layer cobaltite for the Li-ion batteries [3]. In that respect, the intergrowth of well-know structures is an efficient way to generate 2D structures. The Ruddlesden–Popper (RP) series is one well-known example [4] in which the structure can be described as the regular stacking of two types of subcell made of perovskite and rock-salt type layers, respectively.

Increasing n in the generic formula $A_{n+1}M_nO_{3n+1}$ of the RP members (A=Alkaline earth, rare earth, M=transition-metal) allows to go from the A_2MO_4 compounds ($n=1$) with only one perovskite layer to the $n=\infty$ limit term corresponding to the perovskite structure of AMO_3 formula. Furthermore, additional building units can be used in these structures to increase the layering. The use of carbonate groups to separate perovskite layers as in $Sr_2CuO_2(CO_3)$ [5] can be viewed as a way to separate two successive perovskite CuO_2 layers by doing a regular 1:1 stacking of $SrCuO_2$ and $SrCO_3$ layers. Remarkably, such a mechanism can also describe the structure of the $Sr_4M_2O_6CO_3$ oxycarbonates [6–10]: it can be viewed as the $n=3$ member of the RP series for which the central MO_2 layer of the three layer thick perovskite block is replaced by a CO layer. Among the transition metals, layered oxycarbonates have been reported for cuprates including superconducting ones [11], ferrites and mixed ferrites such as Fe/Sc, Fe/Co, Fe/Ni, Fe/Cr and Fe/Mn compounds [6–10]. According to the ability of cobalt cations to adopt different coordination due to spin, charge, and orbital degrees of freedom, there has been a large interest devoted these last years to the cobaltites. At first it is surprising that only one cobalt based oxycarbonate has been reported [12], $Ba_3Co_2O_6(CO_3)_{0.6}$ which structure is not layered but derives from hexagonal perovskite. Nevertheless, several members of the RP cobaltites have been shown to form oxyhydroxydes such as the $n=2$ member $Sr_3Co_2O_5(OH)_2$, xH_2O [13], and $n=3$ member when Co and Ti are mixed as for $Sr_4Co_{1.6}Ti_{1.4}O_8(OH)_2$, xH_2O [14] in which OH groups and H_2O molecules are incorporated at the level of the rocksalt-type block of layers. Thus, we have tried to incorporate triangular CO_3^{2-} carbonate groups to stabilize new layer cobaltites. Using carbonated precursors for solid state reaction in close vessels, a new $Sr_4Co_2(CO_3)O_{6-\delta}$ cobalt oxycarbonate has been prepared. Its structural characterization by means of transmission electron microscopy, X-ray and neutron diffractions reveals that this oxycarbonate is isostructural to $Sr_4Fe_2CO_3O_6$ [7].

2. Experimental

The polycrystalline samples were prepared by mixing SrO, $SrCO_3$, Co_3O_4 and a nearly single phase was obtained starting in

* Corresponding author.
E-mail addresses: denis.pelloquin@ensicaen.fr, pelloquin@ensicaen.fr (D. Pelloquin).

0022-4596/$ - see front matter © 2011 Elsevier Inc. All rights reserved.
doi:10.1016/j.jssc.2011.04.004

3:1:2/3 proportions. SrO was prepared by firstly heating SrO_2 to 873 K and secondly to 1473 K overnight to avoid traces of carbonates and it was then immediately introduced in a nitrogen-filled glove-box to prevent reactivity with ambient atmosphere. The precursors were then weighed and mixed with the other precursors in the glove-box. The intimately ground powders were then pressed in the form of bars, introduced into alumina crucibles and set in silica tubes. The latter were pumped under primary vacuum. After having been taken off the glove-box, they were sealed and then heated up to 1123 K for 24 h and finally quenched to room temperature.

The electron diffraction (ED) and high resolution transmission electron microscopy (HRTEM) studies were carried out with JEOL 2010CX and TOPCON 02B microscopes, respectively. Cation distribution has been checked by energy dispersive spectroscopy (EDS). Both microscopes are equipped with an EDX analyzer. The interpretation of the HRTEM image contrasts was validated with the help of the Mac Tempas Program. The presence of CO_3^{2-} groups was checked by infrared spectroscopy (IR) measurements. Data have been collected in transmission mode, in the range 450–2000 cm^{-1}, with a commercial Nicolet Instrument. Phase purity was also checked by X-ray diffraction using a Panalytical XPert Pro diffractometer equipped with X'Celerator detector and working with Cu $K\alpha$ radiation. Powder neutron diffraction (PND) data were collected at room temperature with the PUS diffractometer at the JEEP II reactor at Kjeller. Neutron with wavelength 1.5554 Å were obtained from a focusing Ge (5 1 1) reflection monochromator. The Fullprof program [15] was used for the Rietveld profile refinements.

3. Structural properties

In order to identify the unit cell and the extinction conditions, an electron diffraction study using a tilt series along the *c*-axis was performed on various crystallites. The basic unit cell was found to be *I*-centered tetragonal, (*h k l*) reflections obeying to *hkl*: $h+k+l=2n$ (Fig. 1), with $a=b\approx 3.8$ Å, $c\approx 28$ Å and $\alpha=\beta=\gamma=90^\circ$. Taking into account this result, the X-ray powder diffraction pattern was fully indexed (Fig. 2) in the *I*4/*mmm* space group with the following cell parameters:

$a = 3.8627(1)$Å and $c = 28.256(1)$Å.

These observations fit well with those usually expected for the $n=3$ member of the RP series, whose theoretical formulation would be $Sr_4Co_3O_{10}$ and *c*-axis parameter ≈ 28 Å (for instance $c\approx 27.2$ Å is reported for $Nd_4Co_3O_{10}$ Ref. [16]). Energy Dispersive Spectroscopy (EDS) analyses were also coupled to electron diffraction for studying more than 20 crystallites. These analyses lead to an average $Sr/Co\approx 2$ cation ratio in agreement with the starting one but much larger than the value of 1.33 expected for an ideal $n=3$ RP member. However, this result is not surprising if we consider the partial substitution of cobalt species by carbonated groups like reported for the iron based oxycarbonate, $Sr_4Fe_2(CO_3)O_6$ [7]. This layer oxycarbonate derives from the stacking mode of the RP $n=3$ member by considering a complete substitution of FeO_6 octahedra by CO_3 triangles in the central layer of the perovskite block. Note that this structure was also refined using a *I*4/*mmm* space group with $a\approx 3.84$ and $c\approx 28.384$ Å [7].

In order to check for the presence of carbonate groups in this cobalt based layered compound, IR measurements were performed. Characteristic peaks of the CO_3^{2-} groups, $\pi(CO_3)$, $\mu_s(CO_3)$ and $\mu_{as}(CO_3)$ are observed on the corresponding spectrum (Fig. 3). Moreover, the $\pi(CO_3)$ bonding confirms that these CO_3 groups are present in the crystallites cores. This strongly supports their incorporation in the crystal structure and supports our structural hypothesis about the formation of an oxycarbonate.

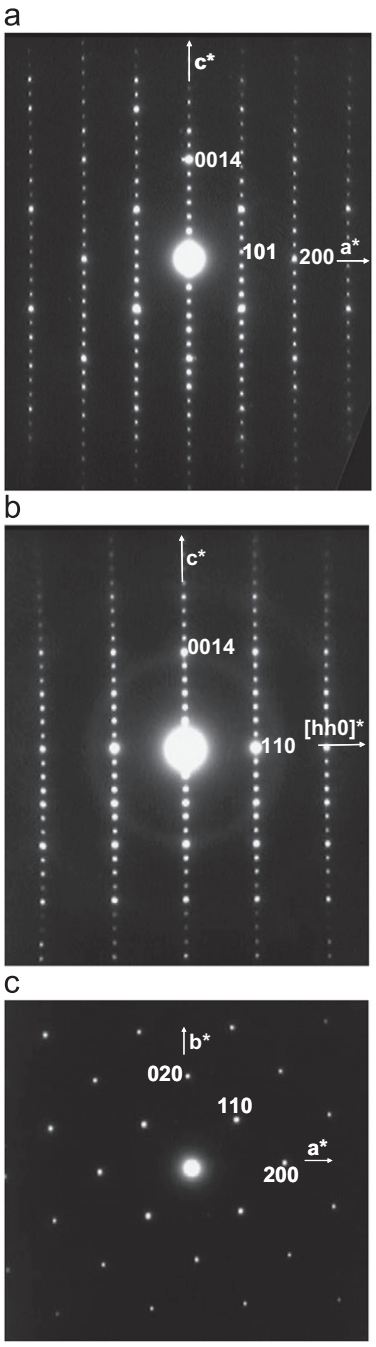

Fig. 1. Experimental electron diffraction patterns collected for $Sr_4Co_2(CO_3)O_{6-\delta}$ with (a) [0 1 0], (b) [−1 1 0] and (c) [0 0 1] zone axis.

As shown previously for different oxycarbonates, the presence of CO_3^{2-} rows in the structure can be revealed by HREM as the CO_3^{2-} contrast differs from those of the other constituting units. A characteristic HREM image recorded for the sample under study is shown in Fig. 4. Assuming that this material has a layered structure deriving from the perovskite structure, the [1 0 0] orientation should allow to visualize the stacking sequence. In the corresponding image (Fig. 4), a part of the contrasts is characteristic of the RP series while the remaining one (white arrow) can be assigned to the presence of carbonate groups. Clearly, this layer stacking is consistent with the structure of the $n=3$ RP member but with carbonate CO_3 substituting the central CoO_6 octhahedra in the perovskite block. A simulated image based on such a model, with an ideal composition "$Sr_4Co_2(CO_3)O_6$" is inserted in Fig. 4. This simulation fits well with the

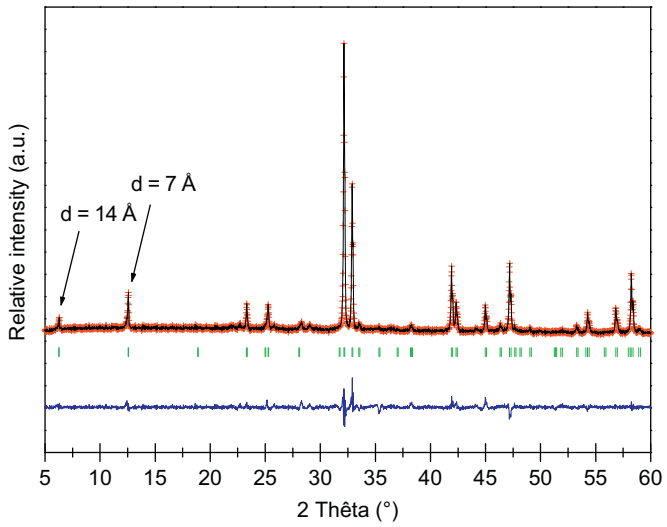

Fig. 2. Experimental powder X-ray diffraction pattern recorded for $Sr_4Co_2(CO_3)O_{6-\delta}$ oxide and indexed in *I*4/*mmm* space group. Arrows pointing at $d_{002}\sim14$ and $d_{004}\sim7$ Å emphasize the comparison with RP3 compounds.

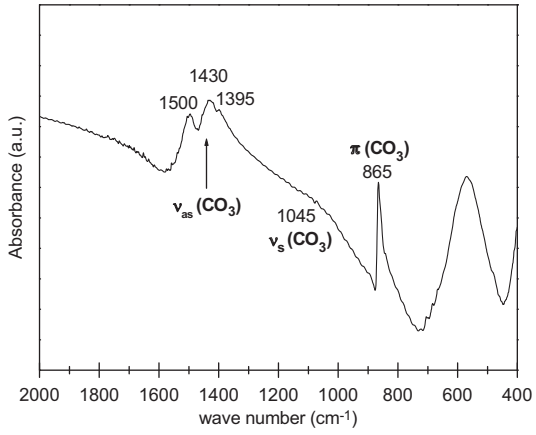

Fig. 3. IR spectra recorded for the $Sr_4Co_2(CO_3)O_{6-\delta}$ oxycarbonate.

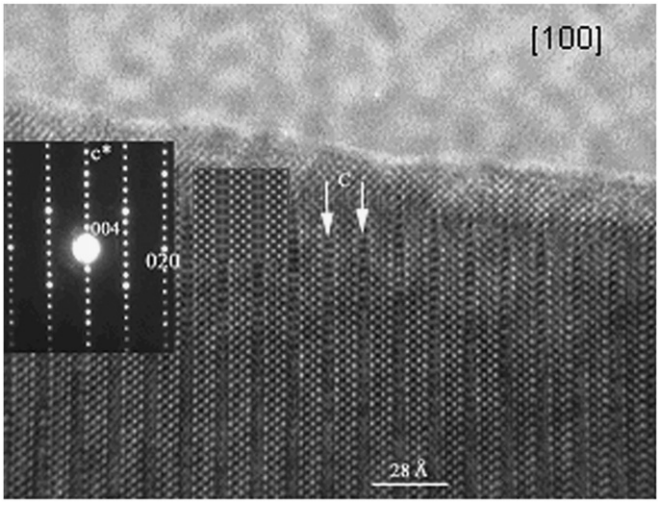

Fig. 4. HREM image and corresponding ED pattern collected along [1 0 0] zone axis. White arrows point on carbonated layers. A simulation, calculated with a crystal thickness close to 3 nm and a defocus value of 50 nm, is inserted.

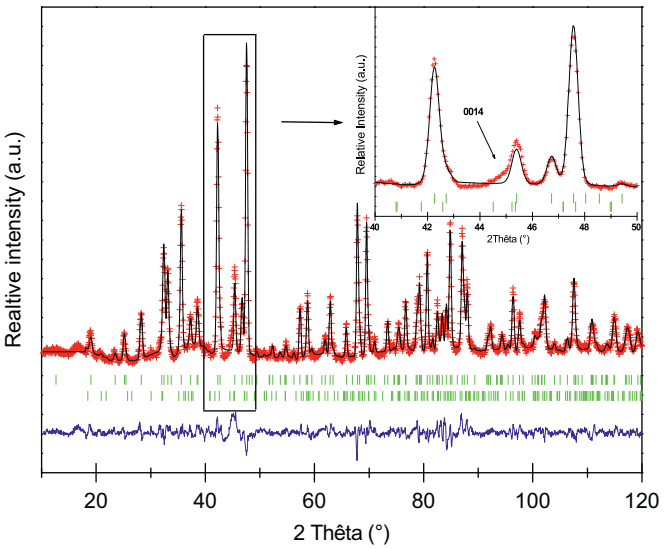

Fig. 5. Experimental, calculated and difference patterns issued from the Rietveld refinements of powder neutron diffraction data. The focused area shows the anisotropic enlargement of 00l reflections with a strong character when sample is exposed in air. The two indexation bars set are related to $Sr_4Co_2(CO_3)O_{5.86}$ and $SrCO_3$ phases respectively.

experimental contrasts. Note that few intergrowth defects have been detected during this work

As both carbon and oxygen are light elements, the structural refinements from X-ray powder diffraction are not accurate enough to establish the structure of this new oxycarbonate. Thus, a powder neutron diffraction experiment at room temperature was performed to refine the structural model established by the previous structural characterizations (Fig. 5). A starting structural model for $Sr_4Co_2(CO_3)O_6$, isostructural to that of $Sr_4Fe_2(CO_3)O_6$ [7], has been used for the Rietveld refinements while $SrCO_3$, detected as impurity during the TEM study, has been introduced as secondary phase. The first refinement converges rapidly for the heavy atoms (Sr,Co) positions as well as for all oxygen except those belonging to the carbonated layers. Similarly to the initial model, the carbon atoms were found to be located on the 2*a* site (0 0 0) of the tetragonal unit cell. Fourier difference maps were then necessary to obtain more informations about neighboring oxygens. Firstly, calculations made without surrounding oxygens revealed the existence of an extra position, O3, located on a 4*e* site, (0 0 *z*) (Fig. 6a). Secondly, taking into account this new O3 position around carbon, refinements were attempted, (Fig. 6b). It is found that the oxygen atoms of the carbonates except the O3 site, can be located on sites with high multiplicity, really close to each other. Moreover, the strong disorder of oxygen atoms, as can be seen on Fig. 6b, suggests that this layer might be relatively flexible compared to the other parts of the structure. Finally, three additional oxygen positions were introduced in the model, namely O4, O5 and O6, corresponding to the highest nucleus densities points near the carbon position. Due to the small occupancy factors of these high multiplicity sites, relatively large errors related to these positions are observed. For the carbonate groups, two dominant configurations are deduced, coat hanger (Fig. 7a) and flag configurations (Fig. 7b).

Hence, considering the difficulty of refining the carbonate layer as aforementioned, the oxygen occupations were constrained to respect the following configurations imposed by the triangularity of the CO_3 group: $n(O4)=2n(O3)$; $n(O6)=2n(O5)$ with a sum of all these oxygens equal to 3 per formula unit. This hypothesis leads to the final model presented in Table 1 with a satisfactory $R_B=0.064$ factor while the amount of $SrCO_3$ phase – detected as impurity – is found close to 4%.

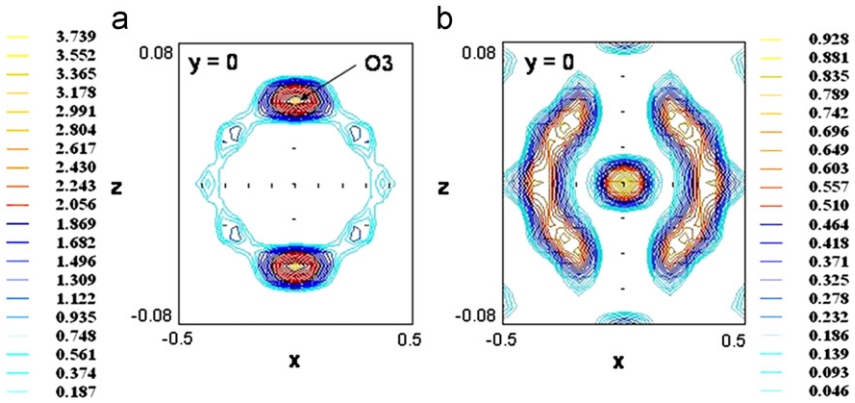

Fig. 6. Fourier difference maps collected to localize oxygen neighboring carbon in the carbonated layers: (a) without oxygen sites around carbon atom and (b) with only O(3) site introduced in refinement.

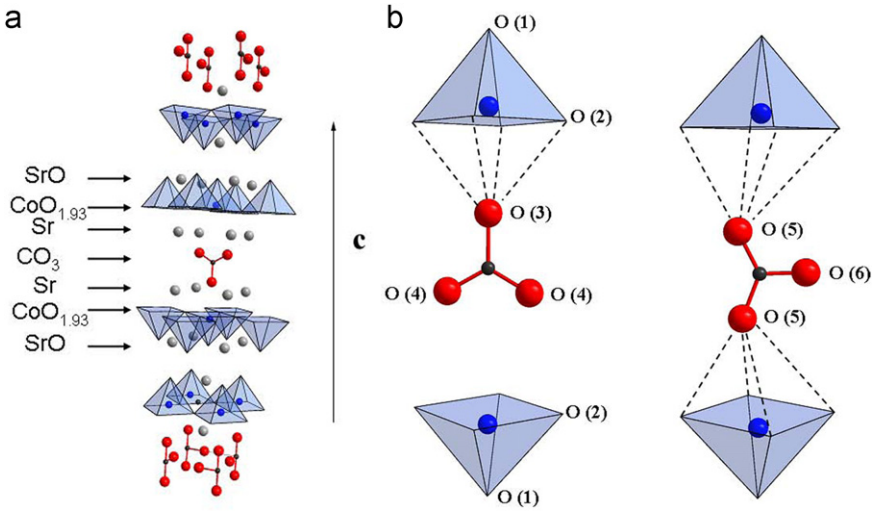

Fig. 7. (a) Structural drawing of the $Sr_4Co_2(CO_3)O_{5.86}$ oxycarbonate. The coat hanger and flag configurations are represented in (b) respectively.

Table 1
Atomic positions of $Sr_4Co_2(CO_3)O_{5.86}$ deduced from final neutron data refinements.

Atoms	Site	x	y	z	B_{iso} (Å^2)	n
Sr(1)	4*e*	0	0	0.5726(2)	0.82(8)	4
Sr(2)	4*e*	0	0	0.7014(2)	0.31(8)	4
Co	4*e*	0	0	0.1426(4)	0.8(2)	4
C	2*a*	0	0	0	0.6(1)	2
O(1)	4*e*	0	0	0.2115(2)	0.38(7)	4
O(2)	8*g*	0	0.5	0.1315(2)	1.17(9)	7.73(9)
O(3)	4*e*	0	0	0.0512(6)	0.3(4)	1.29(4)
O(4)	16*n*	0.295(4)	0	0.0165(6)	0.3(4)	2.57(7)
O(5)	16*n*	0	0.377(10)	0	1.7(5)	0.71(4)
O(6)	8*i*	0.170(9)	0	0.0429(10)	1.7(5)	1.42(7)

$\chi^2=3.00$, $R_{Bragg}=0.0647$, $R_p=0.168$, $R_{wp}=0.164$, $R_{exp}=0.0948$.
Space group: *I*4/*mmm*.
$a=3.86273(2)$, $c=28.2558(2)$.

Table 2
Main atomic distances and angles observed in $Sr_4Co_2(CO_3)O_{5.86}$.

M–O	d (Å) × n[a]	M–O	d (Å) × n[a]
Sr(1)–aO(2)	2.550(3) × 3.88(5)	Co–O(1)	1.95(2) × 1
Sr(1)–O(3)	2.797(4) × 1.29(4)	Co–O(2)	1.96(2) × 3.87(5)
Sr(1)–O(4)	2.620(15) × 1.29(4)	Co–O(3)	2.58(2) × 0.18(2)
Sr(1)–O(5)	2.86(3) × 0.71(4)	Co–O(6)	2.89(3) × 0.35(2)
Sr(1)–O(6)	2.47(3) × 0.71(4)		
		C–O(3)	1.447(17) × 0.65(2)
Sr(2)–O(1)	2.461(5) × 1	C–O(4)	1.229(16) × 1.29(4)
Sr(2)–O(1)	2.746(1) × 4	C–O(5)	1.46(4) × 0.35(2)
Sr(2)–O(2)	2.762(3) × 3.87(5)	C–O(6)	1.37(3) × 0.71(4)
O–C–O (deg) angles			
Triangle O(4)–O(3)–O(4)		Triangle O(5)–O(6)–O(5)	
O(3)–C–O(4)	112(2)	O(6)–C–O(6)	124(3)
O(4)–C–O(4)	135(4)	O(5)–C–O(6)	118(3)

[a] Depending on oxygen occupation sites.

The principal interatomic distances are summarized in Table 2. As shown in Table 1, a small oxygen deficiency is observed in the CoO_2 ideal layers, leading to the actual composition $CoO_{1.93}$. Thus, from these neutron diffraction data refinements the actual formula $Sr_4Co_2(CO_3)O_{5.86}$ is obtained. The structure can be described as that of the $n=3$ member of the RP series, with CO_3 triangles substituting for CoO_6 octahedra in the central layer of the perovskite block.

The small anion deficiency, 0.14 for 6 oxygen atoms, leads to an average cobalt oxidation state close to 2.86. As the cobalt cations can adopt different spin and oxidations states, it is

interesting to compare the Co–O distances with those reported for other cobaltites. In $Sr_4Co_2(CO_3)O_{5.86}$, the majority of the CoO_n polyhedra can be described as square pyramids with four equivalent Co–O distances of 1.96 Å in the basal plane and by a very close apical distance of 1.95 Å. The other Co–O distances, 2.58 and 2.89 Å, are much larger and correspond to a weak bonding to the carbonate groups. This very regular Co–O distances for a fivefold coordinated cobalt contrasts with the anisotropic distances found in oxychlorides [17], Sr_2CoO_3Cl, $Sr_3Co_2O_5Cl_2$ and $Sr_4Co_3O_7 \cdot {}_5Cl_2$, with all basal plane and apical distances in the range 1.97–1.98 and 1.88–1.90 Å, respectively. However, the average Co–O distances for these oxychlorides, ≈1.95 Å, are similar to that found in $Sr_4Co_2(CO_3)O_{5.86}$. On the basis of the 〈Co–O〉 similarity, the cobalt oxidation state of 2.86 deduced from the refined formula appears to be plausible when compared to the trivalent cobalt cations of the oxychlorides [17]. Such a local environment for the cobalt could be consistent with a high spin state for the cobalt species as in Sr_2CoO_3Cl [18]. In that respect, the *z* displacement of the Co in the CoO_5 pyramids is an important parameter. In $Sr_4Co_2(CO_3)O_{5.86}$, the Co cation is off-centered by 0.39 Å which fits well with the Co^{3+} high spin state [18]. However, as there exists oxygen deficiency in the Co^{3+} basal plane [O(2)], some of the cobalt species must adopt a tetrahedral coordination.

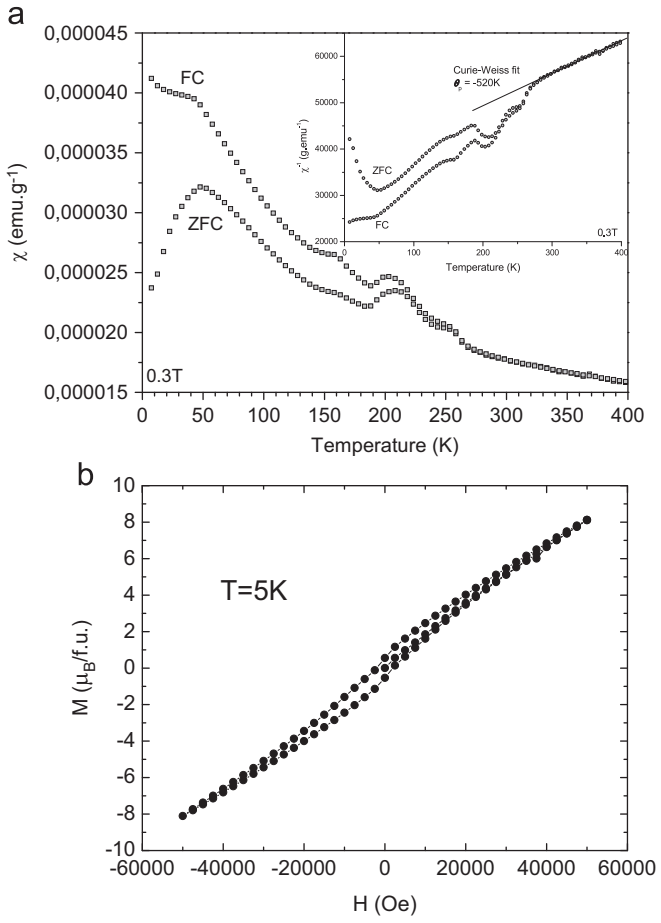

Fig. 8. (a) Magnetic ZFC and FC susceptibility data collected under a field of 0.3 T and (b) M(H) recorded at 5 K of the oxycarbonate $Sr_4Co_2(CO_3)O_{6-\delta}$.

Concerning the carbonate layer, it differs to this one observed in the $Sr_2Cu(CO_3)O_2$ compound. From neutron diffraction data, a single flag configuration more or less tilted is observed in $Sr_2Cu(CO_3)O_2$ [19] while two specific orientations are observed in $Sr_4Co_2(CO_3)O_{5.86}$. Both configurations, coat-hanger and flag, are present in respectively 0.64 and 0.36 proportions which means none of them is strongly favored in this oxycarbonate. Although the $R_{Bragg}=0.0647$ value is quite acceptable, the final profile reliability factor, $R_p=0.163$ can be regarded as too high. It has to be correlated with a degradation of the sample stored in ambient atmosphere conditions that affects mainly the 00*l* reflections, as shown on the enlargement of the Fig. 5. Taking into account our first observations from powder X-ray diffraction evolution, this reaction could be related to a hydration phenomenon as previously reported in the RP oxides [13,14,19,20]. This process that leads to *c*-axis extension in the mentioned examples, although slower in our compound, can explain the anisotropic enlargement of the involved reflections. This reactivity in air will be more completely discussed in a futur paper.

4. Magnetic behavior

The presence of the carbonates as the central layer of the perovskite block, gives to $Sr_4Co_2(CO_3)O_{5.86}$ a very 2D feature. Along the stacking direction, each cobalt is linked through its apical oxygen to the adjacent rocksalt-type layer and separated from the second cobalt layer of the same perovskite block by the carbonate layer (Fig. 7). Accordingly, the main magnetic pathways should be in the basal plane of the CoO_5 square pyramids, i.e. in the (a, b) plane. The O–Co–O angles in these planes being near 180°, one can expect mainly magnetic interactions by super-exchange between nearly trivalent high spin cobalt cations ($S=2$, 4.9 μ_B). In contrast, along the stacking direction, the magnetic

Table 3
Examples of magnetic behaviors of related cobalt oxides and comparison with homologous Fe oxycarbonates and Bi-2201 cobaltite.

Compound	Structure	Co (or Fe) valence	Magnetic properties
$Sr_{1-x}Y_xCoO_3$	Perovskite	2.985 2.865	FM behavior with $T_C \sim 300$ K, but with very small moment [21]
$Sr_3Co_2O_{7-d}$	RP2	Between 2.78 and 3.06	No measurements reported [22]
$Sr_3Co_2O_{5+d}$	RP2	2.91 2.8 2.64 2.38 Hydrated	AFM at 225 K+FM component below 155 K [20] AFM+FM component Two transitions at 170 and 230 K [23] AFM+FM component. One transition at 188 K [20] AFM: two transitions at 120 K and 185 K [20] FM component below ~100 K [20]
$Sr_3Co_2O_5(OH)_2 \cdot xH_2O$	RP2		Canted AFM below 160 K [13]
$Bi_2Sr_2CoO_{6+\delta}$	Bi-2201	Between 2.5 and 3	Phase separation 2D AFM for $\delta \geq 0.4$ with $T_N=235$ K (between Co^{3+} ions) FM component increases as δ decreases below 0.4 (between Co^{2+} and Co^{3+}) [24]
$Sr_4Co_2(CO_3)O_{5.86}$	RP3	2.86	AFM+FM component. Transitions at 50, 160, 210 and 250 K [This work]
$Sr_4Fe_2(CO_3)O_6$	RP3	2.5	3D ordering at 361 K with in plane AFM coupling and out of plane FM coupling [6]
$Sr_4Fe_2(CO_3)O_6$	RP3	2.5	Spin reorientation+structural distortion at 220 K [7]

exchanges must be weaker as they have to be via super-exchange (Co–O–O–Co).

The magnetic behavior has been studied by measuring magnetization (M) as a function of T. The corresponding ZFC and FC curves exhibit a complex evolution with a main peak at 50 K and several others kinds at 160, 210 and 250 K beyond which the both curves start to merge (Fig. 8a). A fit from Curie–Weiss law in the temperature domain ranging from 300 to 400 K lead to $\mu_{eff} \sim 5.7$ $\mu_{B/Co}$ in agreement with the expected value for $Co^{+2.86}$ high spin deduced from structural analyses. According to the χ low values ($\chi = M/H$) and to the corresponding θp ($\theta p = -520$ K), the low temperature transition could indicate an antiferromagnetic state. For comparison, the properties of perovskite and intergrowths related cobalt oxides are reported in Table 3. The AFM behavior observed here is characteristic of these cobaltites with cobalt valency close to 2.8–2.9. For all of them, a ferromagnetic component is also observed as here in the oxycarbonate compound (Fig. 8b). Concerning the values of the transition temperatures, all these cobalt oxides always exhibit two transitions, at ~150 K and one at higher T, close to ~200–230 K. From Table 3, it is obvious that these temperatures do strongly depend on doping. The two transitions observed in $Sr_4Co_2(CO_3)O_{5.86}$ at 160 K and 210 K are close to the ones measured in the $Sr_3Co_2O_{5.91}$ RP2, for a close value of cobalt valency [20]. However this magnetic transition must be considered cautiously since others small peaks are also observed on the $\chi(T)$ curve (Fig. 8a). The origin of these peaks are not clear – intrinsic or due to a small amount of impurities – showing that additional neutron diffraction data to study the magnetic structure at low temperature are absolutely needed to be more affirmative about the magnetism of the $Sr_4Co_2(CO_3)O_{6-\delta}$ phase. Moreover the beginnings of post-synthesis reactivity in air, as hydration mechanism, cannot be excluded like suggested by the degradation of *00l* reflections in time.

5. Concluding remarks

This first work shows again that the use and the control of carbonates is efficient to stabilize new transition metal oxides. This approach using the previous results reported in copper and iron based layered systems has allowed us to discover a new layered cobalt compound. Its structure can be derived from that of the $n=3$ member of the RP series, ideally $Sr_4Co_3O_{10}$, which, to our knowledge, has never been synthesized. The lack of this $n=3$ member might be ascribed to its strong instability or sensitivity in air, which instead leads to the introduction of foreign groups inside the RP3 matrix as illustrated by the stabilization of the oxyhydroxydes $Sr_4(Co,Ti)_3O_{7.5}(OH)_2$, xH_2O [14] and $Sr_3NdFe_3O_{7.5}(OH)_2$, xH_2O [19]. Thus the carbonates substituted at the center of the perovskite block can be seen as an alternative way to successfully stabilize the framework. This oxycarbonate $Sr_4Co_2(CO_3)O_{6-\delta}$ is probably more stable than the hypothetical $Sr_4Co_3O_{10-\delta}$ RP3 member even if its possible post-synthesis reactivity in air is assumed.

From our neutron powder diffraction data collected at RT, no clear magnetic diffraction peaks have been detected. In order to study the magnetic behavior of such carbonated cobaltites, especially below the room temperature, systematic susceptibility measurements will be attempted before and after air exposure starting from freshly prepared $Sr_4Co_{3-x}(CO_3)_xO_{10-4x}$ samples. The crystal chemistry of such a solid solution will give the opportunity to study the structural evolution depending on oxygen stoichiometry/carbonate content and its reactivity in air. All this work is in progress. Additional neutron diffraction data at low temperatures will be also needed to be more affirmative about the magnetic behavior depending on the carbonate content and the fine oxygen stoichiometry.

Acknowledgments

The authors are grateful to Prof. M. Daturi for the IR measurements and the fruitful discussions.

References

[1] J.G. Bednorz, K.A. Müller, Zeitschrift fur Physik B615 (1986) 189.
[2] K. Takada, H. Sakurai, E. Takayama-Muromachi, F- Izumi, R.A. Dilanian, T. Sasaki, Nature 422 (2003) 53.
[3] K. Mitzuchima, P.C. Jone, P.J. Wisemean, J.B. Goodenough, Materials Research Bulletin 15 (1980) 783.
[4] S.N. Ruddlesden, P. Popper, Acta Crystallography 11 (1958) 54–55.
[5] H.G. Von Schnering, M. Hartweg, L. Walz, T. Popp, T. Becker, M. Schwarz, Jahresbericht des MPI für Festkörperforschung Stuggart (1988) 94;
D.V. Fomichev, A.L. Kharlanov, E.V. Antipov, L.M. Kovba, Superconductivity 3 (1990) 126.
[6] K. Yamaura, Q. Huang, J.W. Lynn, R.W. Erwin, R.J. Cava, Journal of Solid State Chemistry 152 (2000) 374–380.
[7] Y. Breard, C. Michel, M. Hervieu, N. Nguyen, A. Ducouret, V. Hardy, A. Maignan, B. Raveau, F. Bouree, G. Andre, Chemistry of Materials 16 (2004) 2895–2905.
[8] Y. Breard, C. Michel, A. Maignan, F. Studer, B. Raveau, Chemistry of Materials 15 (2003) 1273–1282.
[9] Y. Breard, C. Michel, M. Hervieu, A. Ducouret, N. Nguyen, F. Studer, A. Maignan, B. Raveau, E. Suard, Chemistry of Materials 13 (2001) 2423–2429.
[10] Y. Breard, C. Michel, M. Hervieu, N. Nguyen, F. Studer, A. Maignan, B. Raveau, F. Bouree, Journal of Solid State Chemistry 170 (2003) 424–434.
[11] M. Huve, C. Michel, A. Maignan, M. Hervieu, C. Martin, B. Raveau, Physica C 205 (1993) 219–224;
D. Pelloquin, M. Caldés, A. Maignan, C. Michel, M. Hervieu, B. Raveau, Physica C 208 (1993) 121–129.
[12] K. Boulhaya, U. Amador, M. Parras, J.M. Gonzalez-Calbet, Chemistry of Materials 12 (2000) 966.
[13] D. Pelloquin, N. Barrier, A. Maignan, V. Caignaert, Solid State Sciences 7 (2005) 853.
[14] D. Pelloquin, N. Barrier, D. Flahaut, V. Caignaert, A. Maignan, Chemistry of Materials 17 (2005) 773–780.
[15] J. Rodriguez-Carvajal, Physica B 192 (55) (1993).
[16] A. Olafsen, H. Fjellvag, B.C. Hauback, Journal of Solid State Chemistry 151 (2000) 46–55.
[17] S.M. Loureiro, C. Felser, Q. Huang, R.J. Cava, Chemistry of Materials 12 (2000) 3181.
[18] Z. Hu, Hua Wu, M.W. Haverkort, H.H. Hsieh, H.-J. Lin, T. Lorenz, J. Baier, A. Reichl, I. Bonn, C. Felser, A. Tanaka, C.T. Chen, L.H. Tjeng, Physics Review Letters 92 (2004) 207402.
[19] T.G. Narendra Babu, D.J. Fish, C. Greaves, Journal of Materials Chemistry 1 (1991) 677–679;
Y. Miyazaki, H. Yamane, T. Kajitani, T. Oku, K. Hiraga, Y. Morii, K. Fuchizaki, S. Funahashi, T. Hirai, Physica C 191 (1992) 434.
[20] L. Viciu, H.W. Zandbergen, Q. Xu, Q. Huang, M. Lee, R.J. Cava, Journal of Solid State Chemistry 179 (2) (2006) 500–511.
[21] W. Kobayashi, S. Ishiwata, I. Terasaki, M. Takano, I. Grigoraviciute, H. Yamauchi, M. Karppinen, Physical Reveiw B 72 (104408) (2005).
[22] S.E. Dann, M.T. Weller, Journal of Solid State Chemistry (1995) 499–507.
[23] J.M. Hill, B. Dabrowski, J.F. Mitchell, J.D. Jorgensen, Physical Reveiw B 74 (174417) (2006).
[24] K.J. Thomas, Y.S. Lee, F.C. Chou, B. Khaykovich, P.A. Lee, M.A. Kastner, R.J. Cava, J.W. Lynn, Physical Reveiw B 66054415 (2002).